Mineralogical Magazine, February 2016, Vol. 80(1), pp. 127–142

Rare-earth element distribution and genesis of manganese ores associated with Tethyan ophiolites, Iran: A review

Alireza Zarasvandi[1,*], Mohsen Rezaei[1], Martiya Sadeghi[2], Houshang Pourkaseb[1] and Masoume Sepahvand[1]

[1] Department of Geology, Shahid Chamran University (SCU), Ahavz, Iran
[2] Department of Mineral Resources, Geological Survey of Sweden (SGU), Uppsala, Sweden

[*Received 2 March 2015; Accepted 24 November 2015; Associate Editor: Linda Campbell*]

ABSTRACT

The Zagros orogenic and metallogenic belt is characterized by the widespread occurrence of manganese and ferromanganese deposits. These deposits are spatially associated with radiolarian cherts and basaltic rocks, which cap the ophiolite sequences. The present work provides a review on the rare-earth element (*REE*) geochemistry coupled with major- and trace-element geochemical characteristics of the Nasirabad and Abadeh Tashk manganese deposits (associated with the Neyriz ophiolite), and Sorkhvand manganese deposit (associated with the Kermanshah ophiolite). These data are used to gain an insight into the primary ore-forming processes that control the deposition of manganese ores. All of the selected manganese deposits have consistently high Ba contents and low concentrations of trace elements (Co, Cu and Ni) with high Mn/Fe ratios typical of hydrothermal activity. A relatively low *REE* abundance, La_n/Nd_n ratios (>3), and position on a La_n/Ce_n *vs*. $Al_2O_3/(Al_2O_3 + Fe_2O_3)$ discrimination plot indicate a distal hydrothermal source for almost all of the selected manganese deposits. Most of the deposits are characterized by $Ce_{anom} < -0.1$ which reflects the prevailing oxidative conditions during the deposition of manganese ores. Importantly, this is consistent with the occurrence of non-sulfide oxic Mn mineralization in all the manganese deposits of the Zagros orogeny. The comparison of the Sorkhvand, Abadeh Tashk and Nasirabad manganese deposits with other manganese deposits elsewhere in the world indicates that major- and trace-element characteristics, as well as the *REE* composition of the Zagros manganese deposits are analogous to those typical of hydrothermal deposits.

Keywords: manganese, ophiolites, rare-earth elements, Tethys, hydrothermal, Iran.

Introduction

Sedimentary manganese and ferromanganese deposits have a wide distribution in time and space (Roy, 1981). They can form in various environments including continents and on the bottom of the present-day oceans, shallow seas, and lakes (Polgari *et al.,* 2012). Using geochemical parameters marine manganese deposits are classified into four major genetic groups: hydrogenous, diagenetic, hydrothermal and biogenic-bacterial deposits (Oksuz, 2011; Polgari et *al.,* 2012). However, manganese deposits can also form by a combination of these processes (Jach and Dudek, 2005).

Iran is located along the Tethyan suture between Eurasia and Africa – Arabia (Nabatian *et al.,* 2015). More than 45 manganese deposits of economic importance have been reported in Iran (Rezaei, 2012). These deposits have diverse origins and geological settings, and range in age from Precambrian/Early Cambrian to Late Miocene/Pliocene (Shahabpour, 2002; Rezaei, 2012; Ghorbani, 2013; Nabatian *et al.,* 2015). Many of these manganese deposits lie within the Zagros orogenic and metallogenic belt, which is located in the western part of the Tethyan collisional zone. This belt contains excellent exposures of ophiolite sequences, including the Naien, Shahr Babak, Baft,

*E-mail: zarasvandi_a@scu.ac.ir
DOI: 10.1180/minmag.2016.080.054

Neyriz and Kermanshah ophiolites (Fig. 1). The manganese deposits are commonly associated with mudstones, radiolarian cherts and basaltic rocks, capping the ophiolite sequences; examples of such deposits include Abadeh Tashk, Nasirabad (associated with the Neyriz ophiolite), Kamyaran, Sorkhvand (associated with the Kermanshah ophiolites), Gugher and Gushk (associated with the Baft ophiolites). These deposits commonly occur as lenses and small ore beds with a relatively simple mineral paragenesis consisting mainly of pyrolusite and braunite (Rajabzadeh and Zamansani, 2013; Zarasvandi *et al.,* 2014; Sepahvand, 2015). Previous studies have indicated that these deposits are mostly formed by hydrothermal and rarely hydrogenous or diagenetic processes (Rezaei, 2012; Zarasvandi *et al.,* 2013*b*; Rajabzadeh and Zamansani, 2013; Sepahvand, 2015). Although the giant iron and ferromanganese deposits of the Central Iran microcontinent (e.g. Bafq area deposits), east of Central Iran (e.g. Sangan deposit) and the Sanandaj-Sirjan zone (e.g. Gol-e-Gohar deposit) have been the subject of numerous studies (see Ghorbani, 2013; Mohseni and Aftabi, 2015; Nabatian *et al.,* 2015), the overall geological and geochemical features of small-scale

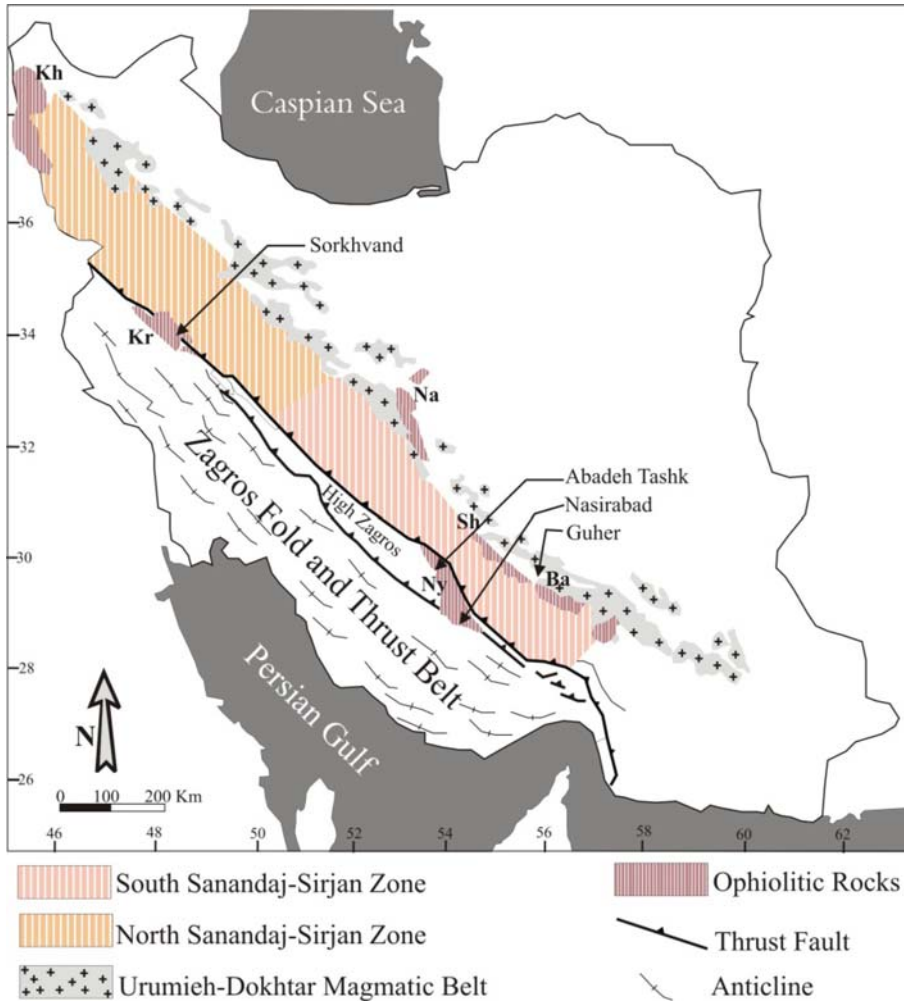

FIG. 1. Map showing locations and distribution of different ophiolite complexes in the Zagros orogeny and the location of the Sorkhvand, Nasirabad, Abadeh Tashk and Gugher manganese and ferromanganese deposits (modified after Ghasemi and Talbot, 2006), Abbreviations; Kh: Khoy, Kr: Kermanshah, Ny: Neyriz, Ba: Baft, Sh: Shahre-Babak, Na: Nain.

https://doi.org/10.1180/minmag.2016.080.054 Published online by Cambridge University Press

TABLE 1. The age (formation) and main characteristics of the Zagros ophiolitic complexes.

Ophiolitic rocks	Formation age	Characteristics
Kermanshah	95–98 Ma (Ar/Ar)[a]	Highly dismembered harzburgite, IAT, OIB[b]
Neyriz	93–95 Ma (Ar/Ar)[c]	Harzburgite, E-MORB (?), IAT[e]
	96–98 Ma (Ar/Ar)[d]	
Nain	99–101 Ma (Ar/Ar)[f]	Harzburgite-lherzolite, small ocean basin around Lut Block[g]
Shahr-e-Babak	93 Ma (Ar/Ar)[h]	Harzburgite-lherzolite, small ocean basin around Lut Block, IAT[h]

[a]Hassanipak *et al.* (2002); [b]Ghazi and Hassanipak (1999); [c]Ghazi et *al.* (1999); [d]Haynes and Reynolds (1980); [e]Sarkarinejad (1994); [f]Hassanipak and Ghazi (2000); [g]Davoudzadeh (1972); [h]Campbell *et al.* (2000).

manganese deposits associated with Tethyan ophiolites of the Zagros orogeny have not been well constrained. Thus, the present work provides a review on the geological and geochemical features of manganese and ferromanganese deposits of the Zagros orogeny. The data are used to provide a general overview on the primary processes that control the deposition of manganese ores.

Regional geology

The Zagros orogenic and metallogenic belt is divided into three major tectonic trends, namely, the Zagros Fold and Thrust Belt (ZFTB), the Sanandaj-Sirjan Metamorphic Zone (subdivided into the North and South SSZ), and the Urumieh-Dokhtar magmatic arc (UDMA)(Alavi, 2004). As depicted by Ghasemi and Talbot (2006), the ophiolitic rocks along the Zagros orogenic belt can be classified into two major groups of different ages: the Nain-Shahr Babak-Baft ophiolite belt, and the Neyriz-Kermanshah ophiolite belt. The former belt is a remnant of the Naien-Baft palaeo-ocean that existed along the northern margin of the South SSZ before the end of the Cretaceous, and the Neyriz-Kermanshah ophiolite belt is a remnant of the Neo-Tethys ocean that was closed during the Miocene (Table 1). The locations of the Sorkhvand, Nasirabad and Abadeh Tashk manganese deposits are shown in Fig. 1. A brief description of selected manganese deposits is presented below.

Local geology

Nasirabad

The Nasirabad manganese occurrence is located to the south of the Neyriz ophiolite. In this region the extremely folded and fractured ore-bearing layers and manganese nodules occur as interlayers with reddish radiolarites in the upper parts of the Pichakun zone. This zone represents the Late Triassic to Middle Cretaceous abyssal facies of the Neo-Tethys ocean basin. It is thought that the Neyriz ophiolite has been thrust over the Pichakun zone (Babaie, 2001). The lower parts of this zone are composed of Upper Triassic megalodon limestone turbidites, dark marl and serpentinite diapirs. These grade upwards into thinly-bedded (<5 cm) cherty radiolarites, alternating with medium- to thick-bedded (up to 5 m) detrital limestone and green siliceous shale. Above this lies a sequence of radiolarites, ~ 500 m thick. Radiolarites of the upper parts, which host the manganese mineralization, are younger than Middle Jurassic in age (Tangestani *et al.,* 2011). Finally, the anhydritic limestone of the Tarbur Formation (Campanian-Maastrichtian) unconformably overlies the radiolarites (Fig. 2*a*). The Nasirabad occurrence is characterized by the absence of Fe ores and the most abundant ore mineral is pyrolusite, occuring as nodules, syngenetic (laminated crusts) and epigenetic (fracture filling) textures (Table 2). Also, syngenetic todorokite minerals have been reported in Nasirabad nodules and ore-bearing layers (Zarasvandi *et al.,* 2013*b*) as a common indication of hydrothermal exhalations (Usui and Someya, 1997). Importantly, syngenetic Mn ores of Nasirabad are characterized by both fine-grained and extended euhedral pyrolusite ore minerals. This feature may indicate the alternative fast and low growth rate and/or precipitation of the manganese oxides of the Nasirabad manganese occurrence.

https://doi.org/10.1180/minmag.2016.080.054 Published online by Cambridge University Press

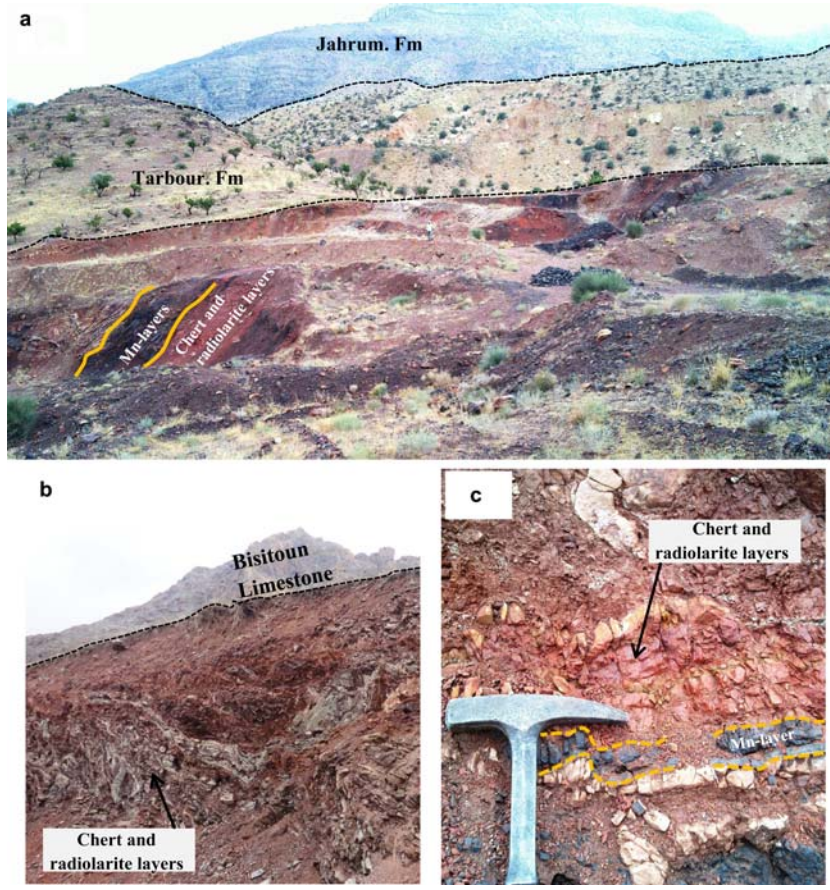

FIG. 2. (*a*) Field photograph of Nasirabad Mn occurrence, showing the Mn-bearing layers and chert with radiolarite layers (photo is looking southwest), (*b*) folding and fracturing in chert and radiolarite layers of Sorkhvand manganese deposit (photo is looking north), (*c*) interlayers of manganese ores and radiolarite cherts in the Sorkhvand manganese deposit.

Abadeh Tashk

The Abadeh Tashk manganese deposits are located to the NE of Tashk lake between 29°47′N and 53°45′E. In this region, the exposure of the Neyriz ophiolite sequence is not complete. The ophiolite forms a discontinuous linear outcrop belt ~16 km long and 11 km wide, between the high Zagros and the main Zagros thrust fault (Fig. 1). Manganese mineraliziation in Abadeh Tashk is associated with radiolarite cherts, belonging to the Late Triassic to Early Cretaceous (Rajabzadeh and Zamansani, 2012). The chert sequences here include both proximal bedded facies, and distal sedimentary facies. However, the bulk of Mn mineralizations are spatially related to reddish brown radiolarian cherts that overlie the serpentinized ultramafic rocks of the ophiolite. These radiolarites are overlain unconformably by massive limestones (Rajabzadeh and Zamansani, 2012). The Abadeh Tashk manganese deposits represent three main textural features including syngenetic, diagenetic and epigenetic types (Rajabzadeh and Zamansani, 2013). The syngenetic textures consist typically of thinly banded (2–3 cm) and disseminated Mn minerals (mainly braunite and psilomelane) within the radiolarite chert interlayers, which cap the pillow lava basalts and serpentinized ultramafic rocks (Table 2). In diagenetic structures, the re-mobilization of ore minerals during deformation events have resulted in accumulation of braunite, pyrolusite and bixbyite in fold hinges (Rajabzadeh and Zamansani, 2013). Moreover, Mn mineralization as lenses and boudin are common features of diagenetic deposits. The epigenetic features represent

https://doi.org/10.1180/minmag.2016.080.054 Published online by Cambridge University Press

TABLE 2. Mineralogical and textural characteristics of the manganese ores associated with Tethyan ophiolites.

Manganese ores	Texture	Major phase	Minor phase
Nasirabad nodules	Zoned, round to elliptical in shape	Quartz and pyrolusite	Todorokite
Nasirabad layers	Laminated and irregular lenses and fractured/folded ore-bearing layers	Quartz and pyrolusite	Todorokite and psilomelane
Sorkhvand	Laminated and/or massive, fracture and fissure filling	Pyrolusite and braunite	Quartz
Abadeh* Tashk	Thinly banded, disseminated and open-space filling	Quartz, pyrolusite and braunite	Hematite, ranceite, psilomelane, aurorite and bixbyite

*Rajabzadeh and Zamansani (2012, 2013).

the post depositional supergene enrichment processes, within which pyrolusite, ranceite and aurorite were mainly deposited as open-space filling textures in the upper parts of chert sequences (Rajabzadeh and Zamansani, 2013).

Sorkhvand

The newly-discovered Sorkhvand manganese deposit is located 30 km southwest of the Harsin, close to the Kermanshah ophiolite in the main Zagros thrust zone (Fig. 1). This ophiolite records the early stage of Neo-Tethys evolution and is composed of mantle metalherzolites, metagabbros and crosscutting metabasaltic dykes, as well as basaltic pillow lavas and dykes (Saccani *et al.,* 2013). In the Sorkhvand deposit, manganese mineralization occurred as irregular lenses or chert interlayers within the Cretaceous radiolarite-bearing mudstones. Towards the northern parts of the deposit, the radiolarites are overlain by a Late Triassic–Late Cretaceous narrow belt of thick, massive, reef-type Bisitoun limestone (Fig. 2*b*). The Mn-rich ores of Sorkhvand have a relatively simple and uniform mineralogy; pyrolusite and braunite occur ubiquitously in the ore samples. No Fe-rich minerals were observed and quartz is the most common gangue mineral similar to those of Nasirabad ore-bearing layers and nodules (Table 2). Three main styles of Mn mineralization are present including: syngeneic (pyrolusite ores); diagenetic (braunite ores); and late-stage epigenetic mineralization (Sepahvand, 2015; Zarasvandi *et al.,* 2014). Syngeneic pyrolusite ore is typically laminated or massive and associated spatially with radiolarite interlayers. The alteration of Mn oxides by silica-rich fluids leads to the development of diagenetic replacement of pyrolusite by braunite minerals along the fault and fractures. Diagenetic braunite is also found as a replacement texture in radiolaria shells, where the silica content of radiolarian shells reacted with ore-bearing fluids. Epigenetic mineralization is found as veinlets of varying thickness formed from the filling of fractures and fissures by pyrolusite ore minerals. In this deposit, silicification as an indication of hydrothermal vents (Jach and Dudek, 2005) leads to the occurrence of jasprite beds throughout the Sorkhvand ore sequences.

Methodology

From the literature data for three manganese deposits were compiled: Sorkhvand, Nasirabad and Abadeh Tashk. For Nasirabad and Sorkhvand, samples were collected from the black chert Mn-bearing layers, nodules and ore layers, respectively. In order to characterize correctly the geochemical features of primary ore-forming processes, unaltered and fractured samples were chosen from syngenetic structures. Accordingly, samples with late-stage diagenetic and epigenetic structures were screened out. Selected samples were crushed using an iron pestle and were subsequently pulverized using a tungsten carbide swing mill. Concentrations of *REE* were obtained by lithium metaborate fusion with nitric digestion followed by inductively coupled plasma mass spectrometry (ICP-MS) and ICP emission spectrometry (ICP-ES) at ACME Analytical Laboratories, Vancouver, Canada. The concentrations of *REE* for the Sorkhvand and Nasirabad samples are given in Table 3. Here samples from Abadeh Tashk were processed by AMDEL Analytical Laboratories (Rajabzadeh and Zamansani, 2013) (Table 3).

https://doi.org/10.1180/minmag.2016.080.054 Published online by Cambridge University Press

TABLE 3. The concentrations of *REE*s (ppm) and some major oxides (wt.%) in the Nasirabad ore-bearing layers, nodules and Abadeh Tashk manganese deposits.

Abadeh Tashk*				Nasirabad Nodules**			Nasirabad Layers				
Sample	1	2	6	N1	N2	N3	LZ-5	LZ-2	La4	LA-10	LA-1
La	<10	<10	<10	2.4	2.5	4.4	6.9	5.8	3	3	5.1
Ce	7.6	8.9	15.4	2	2.4	4.1	11.6	8.5	8.2	5.9	13.2
Pr	0.6	1.22	0.98	0.3	0.33	0.55	1.1	1.17	0.52	0.47	0.98
Nd	3.2	5.96	6.17	0.7	1	1.7	3.6	3.7	1.2	1.5	3.7
Sm	1.12	2.42	1.25	0.15	0.14	0.57	0.81	0.8	0.53	0.28	0.78
Eu	1.42	2.77	0.22	0.04	0.06	0.11	0.19	0.17	0.07	0.07	0.19
Gd	1.69	1.35	1.19	0.21	0.23	0.39	0.8	0.84	0.43	0.25	0.71
Tb	0.11	0.2	0.17	0.03	0.04	0.07	0.12	0.14	0.08	0.05	0.12
Dy	0.45	0.89	0.65	0.15	0.22	0.45	0.82	0.86	0.27	0.2	0.78
Ho	0.13	0.28	0.17	0.05	0.05	0.08	0.16	0.17	0.12	0.04	0.12
Er	0.27	0.51	0.28	0.14	0.15	0.26	0.53	0.39	0.27	0.15	0.38
Tm	0.06	0.13	0.05	0.03	0.03	0.05	0.09	0.06	0.06	0.01	0.06
Yb	0.32	0.6	0.23	0.13	0.15	0.34	0.51	0.39	0.32	0.05	0.45
Lu	0.17	0.12	0.04	0.03	0.03	0.06	0.11	0.06	0.08	0.02	0.07
Σ*REE*	27.14	35.35	36.8	6.36	7.33	13.13	27.34	23.05	15.15	11.99	26.64
Median	0.52	1.05	0.46	0.14	0.15	0.36	0.66	0.59	0.29	0.17	0.58
Ce/La	0.76	0.89	1.54	0.83	0.96	0.93	1.68	1.46	2.73	1.96	2.58
Avg.	1.06			0.9			2.08				
La_n/Nd_n	6.05	3.25	3.13	6.64	4.84	5.01	3.71	3.03	4.84	3.87	2.67
Avg.	4.14			5.49			3.62				
LREE/HREE	7.48	7.66	12.23	7.25	7.14	6.72	7.7	6.92	8.29	14.57	8.9
$(La/Yb)_n$	21.09	11.24	29.34	12.46	11.24	8.73	9.13	10.03	6.32	40.49	7.64
Avg.	20.56			10.81			14.72				
Eu/Eu*	3.15	4.68	0.6	0.68	1.02	0.71	0.72	0.63	0.44	0.8	0.78
Avg.	2.81			0.8			0.67				
Ce_{anom}	–0.41	–0.35	–0.16	–0.38	–0.33	–0.34	–0.13	–0.18	0.01	–0.08	0.00
SiO_2	–	43.22	–	90.0	92.4	93.0	72.6	79.9	90.6	92.0	85.9
TiO_2	–	0.069	–	0.02	0.01	0.01	0.08	0.08	0.05	0.04	0.08
MgO	–	0.1	–	0.09	0.03	0.03	0.20	0.48	0.28	0.21	0.52
MnO_2	–	52.69	–	6.07	4.57	3.7	17.8	10.22	3.22	3.16	4.5
Fe_2O_3	–	1.06	–	0.33	0.33	0.39	0.99	0.95	0.65	0.58	0.11
Al_2O_3	–	0.83	–	0.67	0.48	0.47	1.52	1.74	1.2	0.91	1.8

Na_2O	–	0.39	–	0.08	0.07	0.07	0.15	0.18	0.20	0.14	0.58
K_2O	–	0.11	–	0.06	0.04	0.04	0.15	0.30	0.22	0.12	0.33
CaO	–	0.33	–	0.24	0.19	0.18	0.75	0.95	0.30	0.26	0.57
P_2O_5	–	0.14	–	0.01	0.02	0.01	0.02	0.01	0.02	0.01	0.03

*Rajabzadeh and Zamansani (2013); **Zarasvandi *et al.* (2013*a*).

TABLE 3. (*cont.*)

Sample	SL4L2	SL17L1	Sorkhvand SL20L1	SL16L1	SL4L2–1	SL16L1–1
La	5.6	7.8	5.1	4.2	5.5	4.4
Ce	10	10.8	8.2	5.8	10.4	6
Pr	0.98	1.29	0.87	0.69	0.91	0.72
Nd	3.3	4.3	3.2	3.1	2.8	2.6
Sm	0.66	0.76	0.49	0.48	0.56	0.52
Eu	0.12	0.13	0.12	0.14	0.17	0.17
Gd	0.69	0.9	0.64	0.55	0.71	0.62
Tb	0.15	0.17	0.13	0.11	0.13	0.11
Dy	0.93	0.99	0.92	0.86	0.92	0.77
Ho	0.24	0.28	0.21	0.17	0.22	0.18
Er	0.8	0.81	0.67	0.65	0.7	0.63
Tm	0.13	0.16	0.14	0.12	0.11	0.12
Yb	1.05	1.2	1.1	0.97	1.01	0.94
Lu	0.18	0.21	0.18	0.17	0.19	0.17
Σ*REE*	24.83	29.80	21.97	18.01	24.33	17.95
Median	0.74	0.85	0.65	0.60	0.70	0.62
Ce/La	1.78	1.38	1.60	1.38	1.89	1.36
Avg.	1.56					
La_n/Nd_n	3.2	3.5	3.0	2.6	3.8	3.2
Avg.	3.2					
LREE/*HREE*	4.95	5.31	4.50	4.00	5.09	4.07
$(La/Yb)_n$	3.59	4.38	3.12	2.92	3.67	3.15
Avg.	3.47					
Eu/Eu*	0.54	0.48	0.65	0.83	0.82	0.91

(continued)

TABLE 3. (*contd.*)

Sample	SL4L2	SL17L1	Sorkhvand SL20L1	SL16L1	SL4L2–1	SL16L1–1
Avg.	0.7					
Ce_{anom}	–0.11	–0.20	–0.15	–0.20	–0.09	–0.20
SiO_2	16.21	32.9	6.94	4.03	16.67	3.94
TiO_2	0.01	0.02	0.01	0.01	0.01	0.01
MgO	0.03	0.03	0.02	0.02	0.03	0.02
MnO	56.2	43.8	64.8	67.6	56.8	67.8
Fe_2O_3	0.18	2.36	0.23	0.32	0.33	0.27
Al_2O_3	0.33	0.50	0.26	0.25	0.33	0.25
Na_2O	0.02	0.05	0.01	0.01	0.01	0.01
K_2O	0.05	0.04	0.02	0.01	0.03	0.01
CaO	0.84	0.52	0.35	0.56	0.79	0.57
P_2O_5	0.05	0.06	0.07	0.09	0.07	0.1

Geochemistry

The economic and sub-economic concentration of *REEs* has been demonstrated for a variety of geological settings (Williams-Jones *et al.,* 2000; Migdisov and Williams-Jones, 2014). Rare-earth elements have similar chemical and physical properties but, because of small differences in ionic radius, they may become fractionated relative to each other. Also, the assessment of *REE* geochemistry in ores offers insights into their genesis (Bau and Möller, 1991), with Mn ores being no exception, as has been described for numerous occurrences of modern and ancient ferromanganese deposits in the deep sea and terrestrial environments (e.g. Mishra *et al.,* 2007; Chetty and Gutzmer, 2012). The *REE* data for the Nasirabad ore-bearing layers, nodules, and Sorkhavnd ore samples are listed in Table 3, and compared with data for the Abadeh Tashk manganese deposit. All the ore samples selected are characterized by relatively low *REE* abundance. The median values of *REEs* increase from Nasirabad nodules (0.14–0.36 ppm), to Nasirabad layers (0.17–0.66 ppm), Sorkhvand (0.6–0.85 ppm) and Abadeh Tashk (0.46–1.05 ppm). In general, *REE* distribution patterns exhibit distinct light rare-earth element (*LREE)* enrichment relative to heavy rare-earth element (*HREE*) (Fig. 3), and the $(La/Yb)_n$ value decreases on average from Abadeh Tashk (20.56), to the Nasirabad ore-bearing layers (14.72), Nasirabad nodules (10.81) and Sorkhvand (3.47) respectively. According to Ruhlin and Owen (1986), the pronounced enrichment of the *LREE* relative to *HREE* can be attributed to the greater stability of *HREE* complexes in hydrothermal solutions.

In the present study Cerium (Ce/Ce*) and Europium anomalies (Eu/Eu*) were calculated from: $Ce/Ce^* = Ce_n / (La_n \times Pr_n)^{1/2}$, $Eu/Eu^* = Eu_n / Sm_n \times Gd_n)^{1/2}$ (Taylor and Mclennan, 1985), using chondrite-normalized abundances (Evensen *et al.,* 1978). Taken as a whole, with the exception of the Nasirabad ore-bearing layers, ore samples from the selected areas have negative Ce anomalies (Fig. 3). Moreover, some have weak to strong negative Eu anomalies (avg. Eu/Eu* = 0.67, 0.7 and 0.8 for the Nasirabad ore layers, Sorkhvand and Nasirabad nodules, respectively) whilst some samples of Abadeh Tashk have positive Eu anomalies (Fig. 3, Table 3). It is important to note that the low *REE* concentration, positive Eu anomalies and weak or absent Ce anomalies are considered as common geochemical features of hydrothermal

https://doi.org/10.1180/minmag.2016.080.054 Published online by Cambridge University Press

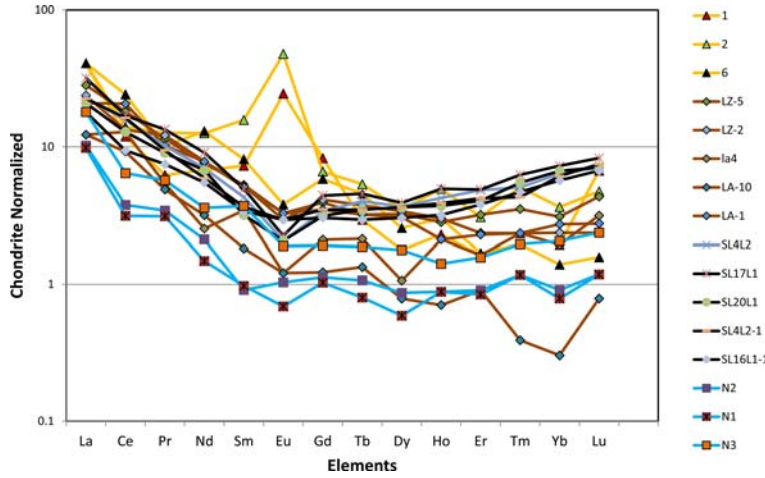

FIG. 3. Chondrite-normalized *REE* patterns of ore samples from the selected areas, with chondrite values from Evensen *et al.* (1978). See Table 3 for sample description.

manganese and ferromanganese deposits (Jach and Dudek, 2005; Xie *et al.,* 2013). In hydrothermal manganese and ferromanganese crusts the La_n/Nd_n ratio is generally between 3.0 and 7.4 (Oksuz, 2011). These ratios in the selected areas are analogous to those typical of hydrothermal crusts and decrease on average from Nasirabad nodules (5.49), to Abadeh Tashk (4.14), Nasirabad ore-bearing layers (3.62) and Sorkhvand (3.2), respectively.

The correlation diagrams indicate that there are strong positive correlations between the *LREE* and *HREE*, suggesting that the same mechanism was responsible for *REE* uptake during the ore formation in all selected manganese and ferromanganese deposits along the Zagros orogen (Fig. 4, Oksuz,

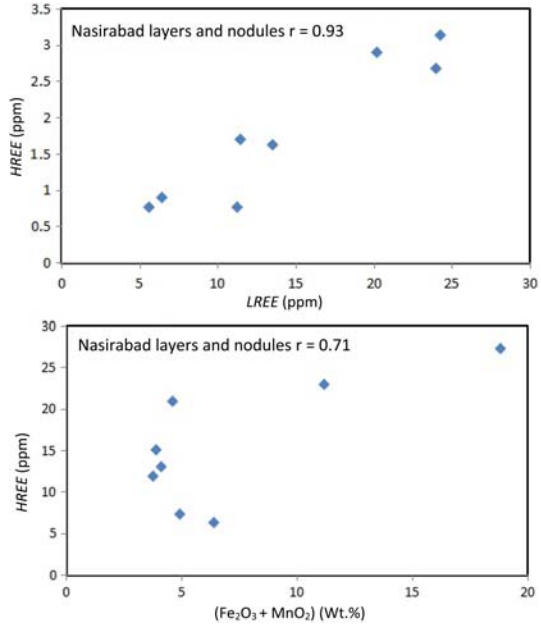

FIG. 4. Examples of good linear correlation between *LREE*, *HREE*, MnO and (Fe_2O_3 + MnO) contents.

https://doi.org/10.1180/minmag.2016.080.054 Published online by Cambridge University Press

2011). Positive correlations were also observed between the Σ*REE* (ppm) and Fe_2O_3 + MnO (wt.%) of samples from the Nasirabad deposit. This feature indicates progressive *REE* scavenging by Mn and Fe oxyhydroxides during the oxidation process (Fig. 4). If we consider a hydrothermal source for mineralization, a relatively weak correlation between Σ*REE* and Fe_2O_3 + MnO may provide insight into the contribution or distortion of *REE* by another source during the Mn mineralization (discussed below).

According to Wright and Holser (1987), the Ce_{anom} [$Ce_{anom.}$= Log $(3 \times Ce_n /(2 \times La_n + Ce_n))$] can be used as a good index for the determination of the oxic or anoxic nature of the water body of sedimentation. An anoxic condition is indicated during sedimentation if $Ce_{anom.} > -0.1$, whereas $Ce_{anom.} < -0.1$ represents oxidative conditions during deposition. The $Ce_{anom.}$ values for the Sorkhvand, Abadeh Tashk and Nasirabad ore bearing layers and nodules are listed in Table 3. With the exception of the Nasirabad ore bearing layers (samples La4, LA-10 and LA-1) and one sample from Sorkhvand (SL4L2-1), all the manganese deposits studied are characterized by $Ce_{anom.} < -0.1$, reflecting oxidative conditions during the deposition of manganese ores.

Maynard (2010) has indicated that Al (and other high-field-strength elements i.e. Zr, Ti, Nb, Y) is insoluble in seawater at surface temperatures and tends not to be fractionated by ordinary geochemical processes in oceanic water. These elements are used as a good indicator for tracing the entrance and/or contribution of detrital materials in manganese mineralization (Mohapatra *et al.,* 2009, Maynard, 2010). There is a significant positive correlation between the Σ*REE* and Al_2O_3 contents of the Nasirabad ore-bearing layers and Sorkhvand, representing the effect or distortion of detrital materials on the *REE* uptake during the formation of Sorkhvand and Nasirabad Mn-bearing layers (Fig. 5). Another indication of this may be seen in the Ce/La values. The Ce/La ratios increase from the Nasirabad nodules (avg. 0.90), to the Abadeh Tashk (avg. 1.06), Sorkhvand (avg. 1.56) and Nasirabad ore-bearing layers (avg. 2.08). According to Dubinin and Volkov (1986), an increasing contribution from carbonaceous biogenic and terrigenous materials can elevate the Ce/La values.

Combining the *REE* results with $Al_2O_3/(Al_2O_3 + Fe_2O_3)$ ratios is useful to delineate the depositional environment of manganese ores (i.e. Xie *et al.,* 2013) in a La_n/Ce_n *vs*. $Al_2O_3/(Al_2O_3 + Fe_2O_3)$ discrimination plot (Murray, 1994). The samples of Zagros manganese deposits are extended between the fields of spreading ridge proximal manganese deposits and a pelagic field (Fig. 6). This feature may indicate a distal hydrothermal source for most of the manganese deposits along the Zagros orogeny.

Discussion

The Zagros orogenic belt is located in the western part of the Tethyan realm. As noted above, two main categories of ophiolitic rocks including

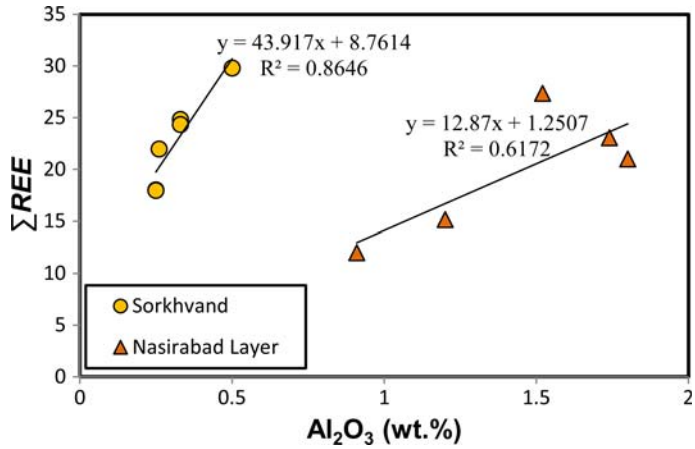

FIG. 5. Strong linear correlation between the Al_2O_3 (wt.%) and Σ*REE* in the Nasirabad ore-bearing layers and Sorkhvand deposit.

https://doi.org/10.1180/minmag.2016.080.054 Published online by Cambridge University Press

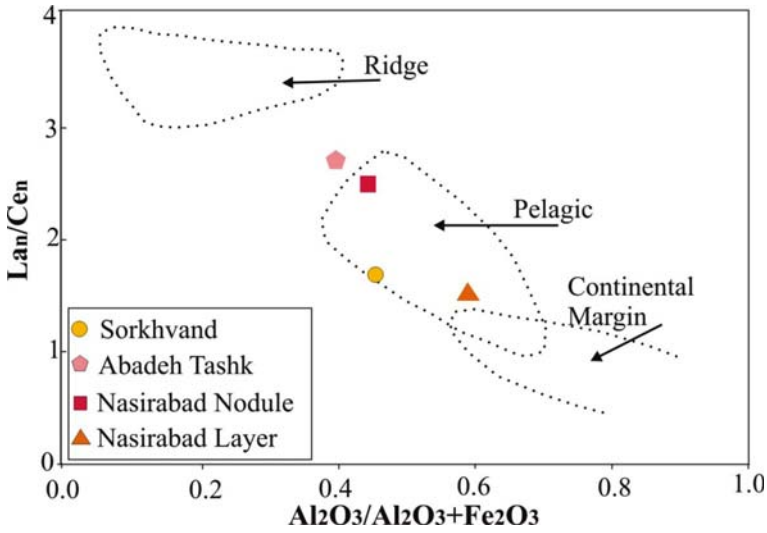

FIG. 6. Plot of La_n/Ce_n *vs*. $Al_2O_3/(Al_2O_3 + Fe_2O_3)$ for the Nasirabad ore-bearing layers and nodules, Sorkhvand and Abadeh Tashk manganese deposits. Modified after Murray (1994). Normalizing values are from (Evensen *et al.,* 1978).

Naien-Shahr Babak-Baft and Neyriz-Kermanshah are situated in this belt (Fig. 1). These ophiolites are characterized by widespread small occurrences of manganese and ferromanganese deposits. However, it is not a unique characteristic, because a wide variety of manganese and ferromanganese deposits have been reported in close association with Tethyan ophiolitic rocks from Cyprus to Pakistan (e.g. Antalya complex, Turkey; northern Apennine ophiolitic complex, Italy; Troodos Massif, Cyprus; Semail nappe, Oman; Wazirestan comlpex, Pakistan). According to Jach and Dudek (2005), marine manganese deposits can be classified into three major genetic groups: hydrothermal, hydrogenous and diagenetic. However, as noted above, Mn mineralization can form by a combination of these processes. Moreover, other parameters such as microbial processes and the selective enrichment of bio-essential elements and contribution of detrital materials can give some distinct geochemical characteristics to manganese and ferromanganese deposits (Polgari *et al.,* 2012; Rezaei, 2012; Zarasvandi *et al.,* 2013*a*). However, previous studies on the geological, mineralogical and geochemical characteristics of Tethyan manganese deposits have indicated that the majority of these deposits were derived originally by hydrothermal processes similar to those of the present-day mid-oceanic spreading centres (see Shah and Khan 1999; Karakus *et al.,* 2010; Oksuz, 2011; Rezaei, 2012; Zarasvandi *et al*., 2013*b*). Here, the overall hydrothermal mineralization model is based on the downwards circulation of seawater through the fractured basaltic oceanic crust. Subsequently, the interaction of seawater with hot basaltic oceanic crust (there are different water/rock ratios) leads to progressive warming and reduction, and increases the acidity of penetrated sea waters (Roy, 1992). These solutions are capable of leaching various elements from basaltic oceanic crust. Finally, the upward re-fluxing of now metal-enriched solutions to the sea water leads to the formation of submarine hydrothermal fluids with high potential for the formation of manganese and ferromanganese deposits.

One of the most common geochemical features of submarine hydrothermal manganese deposits is fractionation of Fe from Mn due to the initial precipitation of Fe-bearing minerals followed by precipitation of Mn-bearing phases (Ruhlin and Owen, 1986; Toth, 1980; Jach and Dudek, 2005). Accordingly, proximal deposits generally exhibit high Fe values, whereas distal deposits are characterized by high Mn content. This feature is evident in the Mn/Fe ratios (Table 4), where almost all of the manganese deposits in the Zagros orogeny display relatively high Mn/Fe ratios which indicate a distal hydrothermal source for Mn mineralization. This characteristic is also reflected in the lack of significant Fe minerals in the selected Mn ores (Table 2). Conformably, high contents of Ba, such as those measured in Zagros manganese deposits

https://doi.org/10.1180/minmag.2016.080.054 Published online by Cambridge University Press

TABLE 4. Comparison between main geochemical features of sub-marine hydrothermal manganese deposits and geochemical characteristics of Zagros manganese deposits.

Hydrothermal geochemical characteristics[a]	Nasirabad Nodules	Nasirabad Layers	Abadeh Tashk	Sorkhvand
High Mn/Fe ratio	13.65	11.96	49.70	207.90
High Ba content (ppm)	879[b]	2209[b]	1363[c]	1684[d]
Co + Cu + Ni < 0.01 (wt.%)	0.01[b]	0.02[b]	0.02[c]	0.04[d]

[a]Jach and Dudek (2005); [b]Rezaei (2012), Zarasvandi *et al.* (2013*b*); [c](Rajabzadeh and Zamansani (2013); [d]Sepahvand (2015).

(Table 4) were reported to occur in deposits from submarine hydrothermal environments (Varnavas *et al.,* 1988; Jach and Dudek, 2005). Hydrothermal geochemical signatures could also be observed in the (Cu + Ni + Co)*10 (ppm) – Fe – Mn (wt. %) ternary diagram (Bonatti *et al.,* 1972; Fig. 7). In this diagram, manganese and ferromanganese ores of the Tethyan realm are characterized by low (Cu + Ni + Co) values (Table 4), and plot collectively in the hydrothermal field (Fig. 7).

The Fe-manganese deposits from Nasirabad, Abadeh Tashk and Sorkhvand are defined by low contents of *REE*, negative Ce anomalies (the Nasirabad ore bearing layers being the exception), *LREE* enrichment relative to *HREE* and La_n/Nd_n values that resemble the composition of hydrothermal manganese deposits formed by low-temperature hydrothermal fluids (Shah and Moon, 2007; Oksuz, 2011; Xie *et al.,* 2013). A comparison of *REE* patterns of Sorkhvand, Aabadeh Tashk and Nasirabad manganese deposits with Tokoro belt hydrothermal deposits (Choi and Hariya, 1992), Peru basin hydrogenous nodules (Von Stackelberg, 1997) and the Eymir deposit (Oksuz, 2011) is shown in Fig. 8. It is evident that the *REE* pattern of manganese deposits associated with Zagros ophiolites is consistent with Tokoro belt and Eymir hydrothermal deposits.

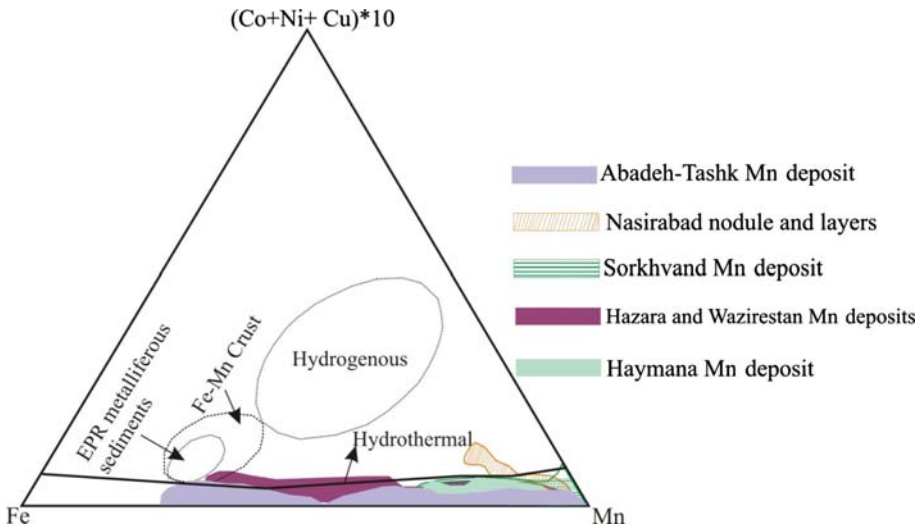

FIG. 7. (Cu + Ni + Co)*10 – Fe – Mn ternary diagram (Bonatti *et al.,* 1972). Field of Abadeh Tashk Mn-deposit from Rajabzadeh and Zamansani (2013), data of Sorkhvand manganese deposit from Sepahvand (2015), field of Nasirabad nodules and Mn-layers after Zarasvandi *et al.* (2013*a*). Data of Wazirestan and Hazara hydrothermal manganese deposits in Pakistan after Shah and Khan (1999) and Shah and Moon (2007), Field of Haymana hydrothermal manganese deposit in Turkey from Karakus *et al.* (2010).

https://doi.org/10.1180/minmag.2016.080.054 Published online by Cambridge University Press

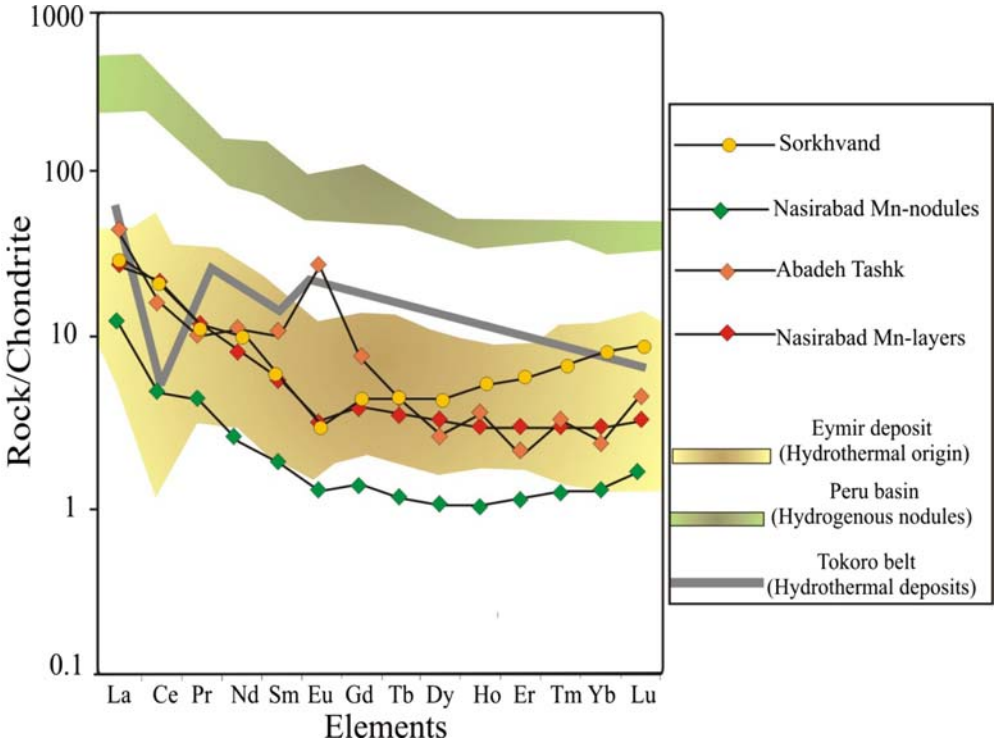

FIG. 8. The compassion of Sorkhvand, Abadeh Tashk and Nasirabad manganese deposits with Tokoro belt hydrothermal deposits (Choi and Hariya, 1992), Peru basin hydrogenous nodules (Von Stackelberg, 1997) and Eymir hydrothermal deposit (Oksuz, 2011).

It has long been recognized that sediments precipitated from hydrothermal vent fluids yield pronounced positive Eu anomalies, with little or no negative Ce anomaly. Also, as pointed out by Michard *et al.* (1993), a Eu anomaly could be a function of high-temperature (>300°C) or low-temperature (<200°C) hydrothermal alteration of the oceanic crust, because high-temperature hydrothermal alteration produces fluids with a pronounced positive Eu anomaly, whereas hydrothermal fluids produced by low-temperature hydrothermal alteration display a weak or no Eu anomalies (Michard *et al.*, 1993). Some samples of Abadeh Tashk exhibit positive Eu anomalies, as is commonly found in hydrothermal settings. In contrast, the Nasirabad and Sorkhvand samples show negative Eu anomalies (Eu/Eu* = 0.68 and 0.7, respectively). Such negative anomalies may result from high dilution of hydrothermal solutions with oceanic water due to the long distance between hydrothermal discharge and depositional environment in the Nasirabad and Sorkhvand deposits (Sabatino *et al.,* 2011). Moreover the lack of volcanic rocks in the vicinity of the Nasirabad and Sorkhvand rock sequences provides further evidence for a remote source for the hydrothermal exhalations (distal hydrothermal source) (Mücke *et al.,* 1999; Zarasvandi *et al*., 2013*a*). Another indication of this conclusion may be seen in the La_n/Ce_n *vs*. $Al_2O_3/(Al_2O_3 + Fe_2O_3)$ discrimination plot (Fig. 6), where average values of Sorkhvand and Nasirabad samples plot in the pelagic field. The contribution of terrigenous materials, especially in the *REE* uptake of Sorkhvand and Nasirabad Mn layers can be traced in the significant positive correlation between Al_2O_3 and Σ*REE* (Fig. 5) and elevated Ce/La values in Sorkhvand and Nasirabad Mn layers. The Sorkhvand and Nasirabad ore bearing layers are characterized by relatively high Ce/La ratios (1.56 and 2.08; respectively). Furthermore, such high Ce/La values and strong linear correlations between Al_2O_3 and Σ*REE* (Fig. 5) may provide an insight into the observed weak positive Ce anomaly in the Nasirabad ore-bearing layers (Fig. 3). The geodynamic setting of Neyriz ophiolite has been discussed in detail by

https://doi.org/10.1180/minmag.2016.080.054 Published online by Cambridge University Press

Shahabpour (2005) and Ghasemi and Talbot (2006). The new geochemical data indicate that Neyriz was an intra-oceanic island arc during the Late Triassic to Late Cretaceous time. Rezaei (2012) and Zarasvandi *et al.* (2013*a b*) pointed out that there are several lines of evidence, including Pb isotopes and major and trace inter-element relations, to show the contribution of mafic terrigenous materials (derived from the eruptions and/or erosion of Neyriz island arc) in the formation of Nasirabad ore sequences.

Summary and conclusion

The remnant of the abyssal facies of Neo-Tethys along the Zagros orogen in Iran is characterized by widespread occurrence of large- to small-scale manganese deposits. These deposits occurred mostly as massive and/or extremely highly-folded and fractured interlayers with radiolarian chert and mudstones. The manganese deposits generally exhibit a simple mineral paragenesis consisting mainly of oxic Mn ores (e.g. pyrolusite and braunite), presenting as primary syngenetic, and late-stage diagenetic and epigenetic structures. Geochemical characteristics of these deposits such as high Mn/Fe ratios and Ba content, together with low *REE* and trace-element content indicate a primary distal hydrothermal source, similar to those of other manganese deposits associated with Tethyan ophiolites in Turkey and Pakistan. However, some distinct characteristics such as elevated Ce/La ratios coupled with a significant correlation between the insoluble elements in hydrothermal systems (e.g. alumina) and the *REE* content of Mn ores in the Sorkhvand and Nasirabad may indicate a minor contribution of detrital materials.

Acknowledgements

This research was made possible by the grant of the office of vice-chancellor for Research and Technology, Shahid Chamran University of Ahvaz in 2015. We acknowledge their support. The authors also would like to thank two anonymous reviewers for the critical and constructive comments which greatly contributed to the improvement of the manuscript.

References

Alavi, M. (2004) Regional stratigraphy of the Zagros fold-thrust belt of Iran and its proforeland evolution. *American Journal of Science*, **304**, 1–20.

Babaie, H.A., Ghazi, M.A., Babaie, A., La Tour, T.E. and Hassanipak, A.A. (2001) Geochemistry of arc volcanic rocks of the Zagros Crush Zone, Neyriz Iran. *Journal of Asian Earth Sciences*, **19**, 61–76.

Bau, M. and Möller, P. (1991) REE systematics as source of information on minerogenesis. Pp. 17–20 in: *Source, Transport and Deposition of Metals* (M. Pagel and J.L. Leroy, editors). Balkema, Rotterdam.

Bonatti, E., Kraemer, T. and Rydell, H. (1972) Classification and genesis of submarine iron–manganese deposits. Pp. 473–489 in: *Ferromanganese Deposits of the Ocean Floor* (D.R. Horn, editor). Harriman, Petersfield, UK.

Campbell, K., Ghazi, A.M., LaTour, T. and Hassanipak, A.A. (2000) Geochemistry, petrology and tectonics of the Shahr-e-Babak ophiolite, SE Iran. *Geological Society of America Annual Meeting, Abstracts with Programs – southeastern Section*, **31**, 9.

Chetty, D. and Gutzmer, J. (2012) REE redistribution during hydrothermal alteration of ores of the Kalahari manganese Deposit. *Ore Geology Reviews*, **47**, 126–135.

Choi, J.H. and Hariya, Y. (1992) Geochemistry and depositional environment of Mn oxide deposits in the Tokoro Belt, Northeastern Hokkaido, Japan. *Economic Geology*, **87**, 1265–1274.

Davoudzadeh, M. (1972) *Geology and Petrology of the area North of Nain, Central Iran.* Report No. 1. Geological Survey of Iran.

Dubinin, A.V. and Volkov, I.I. (1986) Rare earth elements in metalliferous sediments of the East Pacific Rise [J]. *Geokhimija,* **5,** 645.

Evensen, M.N., Hamilton, P. and O'Nions, R.K. (1978) Rare-earth abundances in chondritic meteorites. *Geochimica et Cosmochimica Acta*, **42**, 1199.

Ghasemi, A. and Talbot, C.J. (2006) A new tectonic scenario for the Sanandaj-Sirjan Zone (Iran). *Journal of Asian Earth Sciences*, **26**, 683–693.

Ghazi, A.M. and Hassanipak, A.A. (1999) Geochemistry and petrology of subalkaline and alkaline extrusives of Kermanshah ophiolite, Zagros Suture Zone, SW Iran. *Journal of Asian Earth Sciences*, **17**, 319–332.

Ghazi, A.M., Chatham, B., Hassanipak, A.A., Mahoney, J.J. and Duncan, R.A. (1999) *A petrogenetic investigation of the Khoy ophiolite, NW Iran: implications for Tethyan magmatism and ophiolite genesis. RIDGE Field School: The Troodos Ophiolite and Mid-Ocean Ridge Processes*. Abstract and Field School Notes, Larnaca, Cyprus, July 1999. Oregon State University, USA.

Ghorbani, M. (2013) *The Economic Geology of Iran: Mineral Deposits and Natural Resources.* Springer Geology, 450 pp.

Hassanipak, A.A. and Ghazi, A.M. (2000) Petrology, geochemistry and tectonic setting of the Khoy ophiolite, Northwest Iran. *Journal of Asian Earth Sciences*, **18**, 109–121.

https://doi.org/10.1180/minmag.2016.080.054 Published online by Cambridge University Press

Hassanipak, A.A., Ghazi, A.M., Duncan, R.A., Pessagno, E.A., Kariminia, S.M. and Mobasher, K. (2002) Spatial and temporal distribution of Paleo- and Neo-Tethys ophiolites in Iran and their tectonomagmatic significance. *Geological Society of America Annual Meeting – Abstracts with Programs*, **37**, 33.

Haynes, S.J. and Reynolds, P.H. (1980) Early development of Tethys and Jurassic ophiolite displacement. *Nature*, **283**, 561–563.

Jach, R. and Dudek, T. (2005) Origin of a Toarcian manganese carbonate/silicate deposit from the Krízna unit, Tatra Mountains, Poland. *Chemical Geology*, **224**, 136–152.

Karakus, A., Yavuz, B. and Koc, S. (2010) Mineralogy and major trace element geochemistry of the Haymana manganese mineralizations, Ankara, Turkey. *Geochemistry International*, **48**, 1014–1027.

Maynard, J. (2010) The chemistry of manganese ores through time: a signal of increasing diversity of earth-surface environments. *Economic Geology*, **105**, 535–552.

Michard, A., Michard, G., Stuben, D., Stoffers, P., Cheminee, J.L. and Binard, N. (1993) Submarine thermal springs associated with young volcanoes: the Teahitia vents, Society islands Pacific Ocean. *Geochimica et Cosmochimica Acta*, **57**, 4977–4986.

Migdisov, A.A. and Williams-Jones, A.E. (2014) Hydrothermal transport and deposition of the rare earth elements by fluorine-bearing aqueous liquids. *Mineralium Deposita,* DOI 10.1007/s00126–014-0554-z

Mishra, P.P., Mohapatra, B.K. and Singh, P.P. (2007) Contrasting REE Signatures on Manganese Ore of Iron Ore Group in North Orissa, India. *Journal of Rare Earths*, **25**, 749–758.

Mohapatra, B.K., Mishra, P.P. and Singh, P.P. (2009) Manganese ore deposits in Koira- Noamundi province of iron ore group, north Orissa, India: in the light of geochemical signature. *Chemie der Erde Geochemistry*, **69**, 377–394.

Mohseni, S. and Aftabi, A. (2015) Structural, textural, geochemical and isotopic signatures of synglaciogenic Neoproterozoic banded iron formations (BIFs) at Bafq mining district (BMD), Central Iran: The possible Ediacaran missing link of BIFs in Tethyan metallogeny. *Ore Geology Reviews*, **71**, 215–236.

Mücke, A., Adjimah, K. and Annor, A. (1999) Mineralogy, petrography, geochemistry and genesis of the Paleoproterozoic Birimian manganese-formation of Nsuta/Ghana. *Mineralium Deposita*, **34**, 297–311.

Murray, R.W. (1994) Chemical criteria to identify the depositional environment of chert: general principles and applications. *Sedimentary Geology*, **90**, 213–232.

Nabatian, Gh. Rastad, E., Neubauer, F., Honarmand, M. and Ghaderi, M. (2015) Iron and Fe–Mn mineralization in Iran: implications for Tethyan metallogeny, *Australian Journal of Earth Sciences: An International Geoscience Journal of the Geological Society of Australia,* **62,** 211–241.

Oksuz, N. (2011) Geochemical characteristics of the Eymir (Sorgun-Yozgat) manganese deposit. *Journal of Rare Earths*, **29**, 287–286.

Polgári, M., Hein, J.R., Vigh, T., Szabó-Drubina, M., Fórizs, I., Bíró, L., Müller, A. and Tóth, A.L. (2012) Microbial processes and the origin of the Úrkút manganese deposit, Hungary. *Ore Geology Reviews*, **47**, 87–109.

Rajabzadeh, M.A. and Zamansani, N. (2012) Mineralization study of manganese deposits from Abadeh Tashk area, Fars Province by using mineralogical and geochemical data. *3rd symposium of the Society of Economic geology of Iran, Ahvaz, Iran* [In Persian with English abstract].

Rajabzadeh, M.A. and Zamansani, N. (2013) The investigation of manganese mineralization associted with Neyriz ophiolite melange in the Abadeh Tashk region, Fars province; using mineralogical and geochemical studies. *Iranian Journal of Economic Geology*, **5**, 201–214.

Rezaei, M. (2012) *The Investigation of Geology, Geochemistry and Genesis of Nasirabad Manganese Deposit, Neyriz, Fars province.* Unpublished MSc dissertation, Shahid Chamran University, Ahvaz, Iran.

Roy, S. (1981) *Manganese Deposits.* Academic Press, London, 458 pp.

Roy, S. (1992) Environment and processes of manganese deposition. *Economic Geology*, **87**, 1218–1236.

Ruhlin, D.E. and Owen, R.M. (1986) The rare earth element geochemistry of hydro-thermal sediments from the East Pacific Rise: examination of a seawater scavenging mechanism. *Geochimica et Cosmochimica Acta*, **50**, 393–400.

Sabatino, N., Neri, R., Bellanca, A., Jenkyns, H.C., Masetti, D. and Scopelliti, G. (2011) Petrography and high-resolution geochemical records of Lower Jurassic manganese-rich deposits from Monte Mangart, Julian Alps. *Palaeogeography, Palaeoclimatology, Palaeoecology*, **299**, 97–109.

Saccani, E., Allahyari, Kh., Beccaluva, L. and Bianchini, G. (2013) Geochemistry and petrology of the Kermanshah ophiolites (Iran): Implication for the interaction between passive rifting, oceanic accretion, and OIB-type components in the Southern Neo-Tethys Ocean. *Gondwana Research*, **24**, 392–411.

Sarkarinejad, K. (1994) Petrology and tectonic setting of the Neyriz ophiolite, southeast Iran. Pp. 221–234 in: *Circum-Pacific Ophiolites* (A. Ishiwatari, A. Malpas and H. Ishizuka, editors). Proceedings, 29th International Geological Congress, Part D. VSP, Utrecht, The Netherlands,

Sepahvand, M. (2015) *Geology, geochemistry and genesis of Sorkhvand manganese deposit, SW Harsin,*

https://doi.org/10.1180/minmag.2016.080.054 Published online by Cambridge University Press

Kermanshah. Unpublished MSc dissertation, Shahid Chamran University, Ahvaz, Iran.

Shah, M.T. and Khan, A. (1999) Geochemistry and origin of Mn-deposits in the Waziristan ophiolite complex, north Waziristan, Pakistan. *Mineralium Deposita*, **34**, 697–704.

Shah, M.T. and Moon, C.J. (2007) Manganese and ferromanganese ores from different tectonic settings in the NW Himalayas, Pakistan. *Journal Asian Earth Science*, **29**, 455–465.

Shahabpour, J. (2002) *Economic Geology,* **137,** 543, Shahid Bahonar University of Kerman Publications [in Persian].

Shahabpour, J. (2005) Tectonic evolution of the orogenic belt in the region located between Kerman and Neyriz. *Journal of Asian Earth Science*, **24**, 405–417.

Stocklin, J. (1974) Possible ancient continental margine in Iran. Pp. 873–887 in: *The Geology of Continental Margins* (C.A. Burke and C.L. Drake, editors). Springer, New York.

Tangestani, M., Jaffari, L., Vincent, R. and Maruthi Sridhar, B.B. (2011) Spectral characterization and ASTER-based lithological mapping of an ophiolite complex: A case study from Neyriz ophiolite, SW Iran. *Remote Sensing of Environment*, **115**, 2243–2254.

Taylor, S.R. and Mclennan, S.M. (1985) *The Continental Crustal: Its Composition and Evolution.* Blackwell, Oxford, UK, 312 pp.

Toth, J.R. (1980) Deposition of submarine crusts rich in manganese and iron. *Geological Society of America Bulletin*, **91**, 44–54.

Usui, A. and Someya, M. (1997) Distribution and composition of marine hydrogenetic and hydrothermal manganese deposits in the northwest Pacific. Pp. 177–198 in: *Manganese Mineralization: Geochemistry and Mineralogy of Terrestrial and Marine Deposits* (K. Nicholson, J.R. Hein, B. Buhn and S. Dasgupta, editors). Geological Society, London, Special Publications, **19**.

Varnavas, S.P., Papaioannu, J. and Catani, J. (1988) A hydrothermal manganese deposit from the Eratosthenes Seamount, eastern Mediterranean Sea. *Marine Geology*, **81**, 205–214.

Von Stackelberg, U. (1997) Growth history of manganese nodules and crusts of the Peru basin. Pp. 153–176 in: *Manganese Mineralization: Geochemistry and Mineralogy of Terrestrial and Marine Deposits* (K. Nicholson, J.R. Hein, B. Bühn and S. Dasgupta, editors). Geological Society, London, Special Publications, **119**.

Williams-Jones, A.E., Samson, I.M. and Olivo, G.R. (2000) The genesis of hydrothermal fluorite-REE deposits in the Gallinas Mountains, New Mexico. *Economic Geology*, **95**, 327–341.

Wright, J. and Holser, W.T. (1987) Paleoredox variations in ancient oceans recorded by rare earth elements in fossil apatite. *Geochimica et Cosmochimica Acta*, **51**, 631–644.

Xie, J., Sun, W., Du, J., Xu, W., Wu, L., Yang, S. and Zhou, S. (2013) Geochemical studies on Permian manganese deposits in Guichi, eastern China: Implications for their origin and formative environments. *Journal of Asian Earth Sciences*, **74**, 155–166.

Zarasvandi, A., Lentz, D., Rezaei, M. and Pourkaseb, H. (2013*a*) Genesis of the Nasirabad manganese occurrence, Fars province, Iran: Geochemical evidences. *Chemie der Erde Geochemistry*, **73**, 495–508.

Zarasvandi, A., Rezaei, M., Pourkaseb, H. and Saki, A. (2013*b*) Investigation on primary and secondary processes in Nasirabad manganese deposit, south of Neyriz: using mineralogy and Pb isotope geochemistry. *Iranian Journal of Economic Geology*, **5**, 37–47.

Zarasvandi, A., Sepahvand, M., Pourkaseb, H. and Rezaei, M. (2014) Mineralogical and textural studies on the Sorkhvand manganese deposit, Harsin: Evidences for ore forming processes. *6th Symposium of the Society of Economic Geology of Iran.* Zahedan, Iran.

https://doi.org/10.1180/minmag.2016.080.054 Published online by Cambridge University Press